Estimation of an Effective Water Diffusion Coefficient During Infrared-Convective Drying of a Polymer Solution

N. Allanic
OPERP ERT 1086, GEPEA, Université de Nantes – IUT de Nantes, 2 avenue du Professeur Jean Rouxel, 44475 Carquefou Cedex, France

P. Salagnac
Laboratoire d'Etude des Phénomènes de Transfert et de l'Instantanéité: Agro-ressources et Bâtiment (LEPTIAB) Université de La Rochelle, Avenue Michel Crépeau, F-17042 La Rochelle Cedex 1, France

P. Glouannec
Laboratoire d'Ingénierie des Matériaux de Bretagne (LIMATB), équipe ETEE, Université Européenne de Bretagne, Rue Saint-Maudé, B. P. 92116, 56321 Lorient Cedex, France

B. Guerrier
Univ Pierre et Marie Curie-Paris 6, Univ Paris-Sud, CNRS, Lab FAST, Bat 502, Campus Univ, Orsay, F-91405, France

DOI 10.1002/aic.11877
Published online July 16, 2009 in Wiley InterScience (www.interscience.wiley.com).

This article deals with the drying of an aqueous solution of polyvinyl alcohol mixed with a plasticizer. A heating combining forced convection and short-infrared radiation was investigated. A one-dimensional model taking into account the shrinkage of the product was developed to get the temperature and moisture content evolutions during the drying. The water diffusion coefficient was estimated by an inverse method. A sensitivity analysis and numerical tests showed the relevance of using an objective function taking both mass and temperature measurements into account for the estimation procedure. This estimation was performed on several convective and infrared-convective experimental drying kinetics. The model predictions fit well mass and temperature experimental data.
 AIChE J, 55: 2345–2355, 2009
Keywords: polyvinyl alcohol, drying, infrared heating, inverse method, mass diffusion coefficient

Introduction

Mechanisms involved in industrial polymer drying processes have been investigated in many experimental and theoretical studies.[1] Because of new environmental norms, the use of volatile organic solvents is being reduced in favor of water solutions.[2] The energy needed to evaporate water is greater than for classical organic solvents, therefore energy requirements must be optimized. One possibility is to use infrared technologies, which allow a direct transfer of a greater amount of energy to the product. However, polymer solutions are very sensitive to temperature, they undergo a high shrinkage and their physicochemical properties evolve with moisture content throughout the drying process,[3,4]

Correspondence concerning this article should be addressed to N. Allanic at nadine.allanic@univ-nantes.fr

Table 1. Material Properties (PVA/Glycerol/Water)

Properties	
Density and linear shrinkage coefficient	$\rho_B^0 = 1300$ kg m^{-3} and $\psi = 1.3$
Glass temperature transition	$T_{g,B} = 51°C$
Activity	$X = \frac{W_m CKa_w}{(1-Ka_w)(1-Ka_w+CKa_w)}$ $C = 2.2723$, $K = 0.9382$, and $W_m = 0.1933$

which may induce the formation of bubbles, cracks, or skin at the surface of polymer materials.[5,6] To avoid product damages, it is then necessary to carefully control energy input, particularly in the case of infrared drying.

The work presented in this article is a first step to the optimization of an industrial drying process combining forced convection and short-infrared radiation, the aim of which is to decrease the drying time, improve the quality of the final product, and minimize energy consumption. The product is an aqueous polymer solution with a high initial moisture content ($X = 7.5$ kg kg^{-1} per dry basis), a high initial thickness (1.3 mm), and is dried in a Petri dish. The aim was not to have a very low final moisture content of the product but to tend to $X = 1$ kg kg$^{-1.}$ without exceeding a 90°C temperature. This configuration is quite different of usual coating processes, in which products have low initial thicknesses (about a few hundred micrometers) and are often coated on metallic substrates.[3,7] Moreover, contrary to many paintings or varnishes, no reticulation phenomena are involved. The dried polymer film is used to perform biochemical analyses in sterile atmosphere.

To be able to optimize the drying process, it is necessary to have a good knowledge of the product drying behavior and of the evolution of the mutual diffusion coefficient with water content. Indeed, for low-moisture content, and when the activity begins to decrease, drying is no longer controlled by evaporation but is limited by water diffusion in polymer. It is well known that diffusion coefficients decrease by several orders of magnitude during drying. Direct experimental determination is difficult for the whole range of concentration involved during drying.[8] Theoretical approaches have been investigated such as the free-volume theory,[3] but they involve a lot of physico-chemical properties, which are generally poorly characterized, especially for complex solutions or industrial products. As a consequence, several authors have suggested estimating an effective diffusion coefficient by means of an inverse method from experimental drying kinetics.[9,10] The diffusion coefficient is generally expressed by an exponential dependence with temperature and concentration.[7,11] Coupling experimental kinetics, simulation of the drying, and an optimization procedure, the authors determine the unknown parameters of the exponential law. In most of these studies, only convective drying experiments are involved and only mass measurements are performed.[9] In the present work, both convective and infrared drying kinetics are considered. The approach used to estimate the effective diffusion coefficient is detailed for the industrial application underlying this study. However, the developed methodology could easily be extended to other configurations. A sensitivity analysis is performed to characterize the feasibility of the estimation and the relevance of using both mass and temperature data is discussed.

Material and Experimental Setup

Material properties

The solution has an initial 88% water mass fraction. The polymer is a poly(vinyl alcohol) (PVA) partially hydrolyzed (80%). A plasticizer (glycerol) is introduced in the solution in the same mass proportion than the PVA. Because of its physicochemical properties,[12] we assumed that the glycerol does not evaporate during drying. Most of the physical properties of the product were experimentally measured. To verify that the shrinkage can be expressed linearly as a function of the moisture content (linear shrinkage coefficient ψ), the density of a pure PVA solution was measured for several volume fractions.[13] The water activity was obtained from sorption isotherms and expressed by the GAB model.[14] By means of a differential scanning calorimeter, we obtained the evolution of the heat specific capacity of the dried product and its glass transition temperature. To characterize the percentage of infrared irradiation absorbed by the product during drying, its transmitivity was measured in the visible and infrared wavelength range with an infrared spectrometer. An average absorption coefficient was deduced from theses measurements and expressed as a function of the moisture content and thus of the thickness.[15] The main properties of the studied product are given in Table 1.

Experimental setup

A drying pilot combining convective drying with short infrared irradiation[16] was used (cf. Figure 1). In this pilot, the air temperature and velocity are regulated, whereas humidity is only measured. The product was dried in a Petri dish. Therefore, the product temperature was measured at the surface by an optical pyrometer (T_{surf}) and on the upper side of the bottom of the Petri dish (T_{bu}) by a thermocouple. The temperature uncertainty is ±2.5°C. An electronic scale is used to measure the product mass as a function of time, with uncertainty of ±0.2 g. In a previous work,[15] many convective drying experiments were carried out by changing the air velocity (1–2.8 m s^{-1}) and the air temperature (35–55°C). For convective-infrared drying, the infrared irradiation evolved between 3.7 and 16 kW m^{-2}, whereas aeraulic conditions were constant ($T_{air} = 35°C$ and $v_{air} = 1$ m s^{-1}). All these tests showed the interest of infrared irradiation to decrease drying time compared with classical convective drying. But careful regulation is needed to avoid product

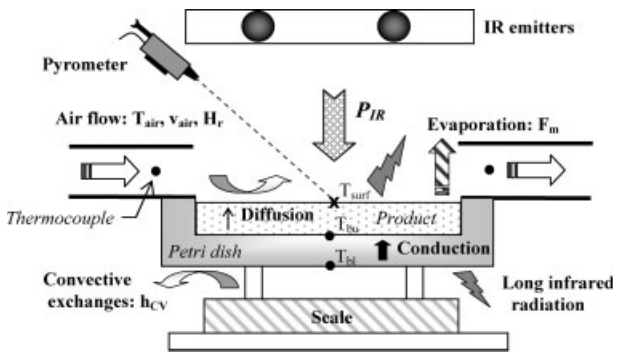

Figure 1. Heat and mass transfers.

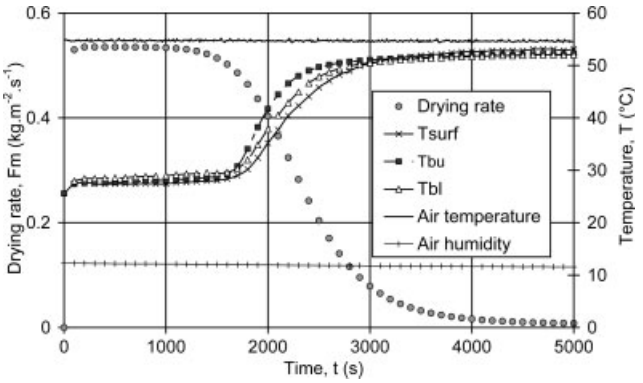

Figure 2. Convective drying kinetics (T_{air} = 55°C, v_{air} = 1.5 m s^{-1}, H_R = 11%).

damage.[15] Figure 2 shows an example of experimental results obtained with an air flow velocity of 1.5 m s^{-1} and an air temperature of 55°C. In this experiment, air humidity was nearly constant and around 11%.

Model

The one-dimensional physical model based on mass and energy balances[17] gives temperature (T) and moisture content (X) evolutions. We assume that the evaporation of water occurs only at the surface of the product and that it remains in a rubbery state throughout the drying process (i.e., no glass transition). As already said, the shrinkage of the product was assumed linear:

$$e = e_d(1 + \psi X_m) \tag{1}$$

with ψ the linear shrinkage coefficient.

Heat and mass transfer equations

Mass Balance. The mass conservation equations of water and polymer, respectively, noted as A and B are written as[18]:

$$\begin{cases} \dfrac{\partial \rho_B}{\partial t} + \dfrac{\partial}{\partial z}(\rho_B v) = \dfrac{\partial}{\partial z}\left(\rho D \dfrac{\partial}{\partial z}\dfrac{\rho_B}{\rho}\right) \\ \dfrac{\partial \rho_A}{\partial t} + \dfrac{\partial}{\partial z}(\rho_A v) = \dfrac{\partial}{\partial z}\left(\rho D \dfrac{\partial}{\partial z}\dfrac{\rho_A}{\rho}\right) \end{cases} \tag{2, 3}$$

where D is the mutual diffusion coefficient and v is an average of the velocities of each constituent.

Two approaches, respectively, based on the barycentric velocity and on the volume velocity, are classically used to describe mass transfers.[19,20] In both cases, a suitable change of variables is used to avoid numerical difficulties related to the moving front (cf. Figure 3). In the barycentric approach, the mass balance is rewritten in the dried product domain thanks to an Eulerian-Lagrangian transformation.[21] In this case, the velocity of the dried product is 0 and the space variable (ξ) evolves in a fixed domain between 0 and the dried product thickness (e_d). Considering a volume velocity, the domain variation is taken into account by means of a Landau transformation[22,23] which enables to have a fixed domain between 0 and 1. With the Landau transformation, integrating Fick's law onto surface involves the presence of the diffusion coefficient in the denominator. Because of the strong variation of the diffusion coefficient with the water content, this approach needs a very small spatial grid near the interface, where the concentration gradient is very large, to ensure numerical convergence.[23] Preliminary numerical tests have been performed to compare both methods, using the same diffusion coefficient (i.e., neglecting the density difference between the two components). Similar results were obtained. As the barycentric approach needs a less refined mesh, it was used in the following.[13] By introducing the moisture content $X = \frac{\rho_A}{\rho_B}$ and combining the Eqs. 2 and 3, the diffusion equation can be written in the Lagrangian domain ($0 < \xi < e_d$):

$$\frac{\partial X}{\partial t} = \frac{\partial}{\partial \xi}\left(\frac{D}{(1+\psi X)^2}\frac{\partial X}{\partial \xi}\right) \tag{4}$$

At $\xi = 0$ (Figure 3), the product is in contact with the Petri dish and the surface is impermeable. At the product–air interface, corresponding to $\xi = e_d$, the mass balance is expressed by[21]:

$$F_m(1+\psi X)^2 = -D\rho_B^0 \frac{\partial X}{\partial \zeta} \tag{5}$$

where ρ_B^0 is the intrinsic density of the polymer constituent.

In this equation, the drying rate is:

$$F_m = k_m\left(\frac{P_t M_v}{RT}\right)\ln\left(\frac{P_t - P_{vair}}{P_t - a_w P_{vsat}(T)}\right) \tag{6}$$

with a_w the water activity and k_m the mass transfer coefficient which depends on the heat convective exchange coefficient (h_p).

Thermal Balance. Experimental data show that the difference between the surface temperature (T_{surf}) and the bottom temperature (T_{bu}, cf. Figure 1) is always small.[15] Thus, the temperature of the polymer solution was assumed uniform, as often in the literature.[22,23] The thermal balance was written in the following way:

$$(\rho C_p e)\frac{\partial T}{\partial t} = h_p(T_{air} - T) - F_m L_v + \varepsilon\sigma\left(T_{wall}^4 - T^4\right) + \phi_b + \phi_{IR} \tag{7}$$

where T is the solution temperature.

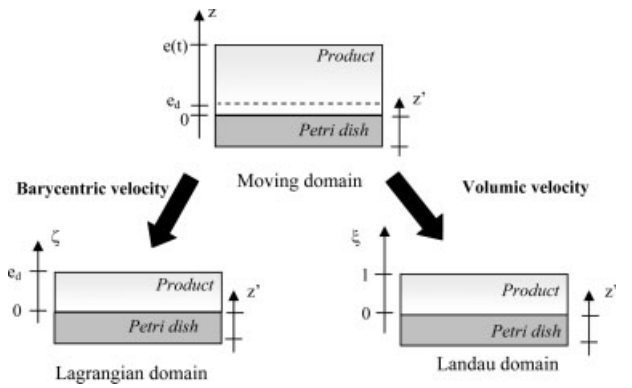

Figure 3. Fixed and moving numerical domains.

ϕ_{IR} is the absorbed short wave infrared irradiation (semi-transparent medium) given by the Lambert-Beer law.[24]

ϕ_b corresponds to the conductive heat exchange with the substrate (Polystyrene Petri dish). It is obtained by solving the heat balance in the Petri dish, which takes into account conduction transfer and short wave infrared input. On the lower side, the Petri dish was exposed to free convective and long wave radiative exchanges. Heat and mass transfers and boundary conditions, which are involved in the convective-infrared drying, are shown in Figure 1.

Numerical procedure

The differential equations concerning the mass balance and the heat transfers in the product were spatially integrated by a control volume method.[25] All the equations were simultaneously solved by means of a predictor-corrector method with a high order. The coupling and the nonlinearity of equations were solved by a Newton method.[26] Fifty control volumes were considered in the polymer and five control volumes in the Petri dish. A convergence criterion of 10^{-3} was introduced. The time step was variable to assure the convergence of calculus.

Estimation of the Effective Diffusion Coefficient

Several expressions of the dependence of the diffusion coefficient on moisture content or solvent concentration can be found in literature. Some of them, like those suggested by Yoshida and Miyashita[27] or Vrentas and Vrentas,[28] are based on the free-volume theory. Others take into account the change of the diffusion coefficient at the glass transition[11,29] or induced by the crystallinity of the polymer notably for PVA.[30,31] The influence of temperature on the diffusion coefficient is generally described by an Arrhenius law with a constant activation energy. In the following, to limit the number of parameters to be estimated, the diffusion coefficient was expressed as an exponential function of temperature and moisture content[7,21]:

$$D(X,T) = D_0 e^{-\frac{E_a}{RT}} e^{-\frac{a}{X}} \tag{8}$$

where E_a is the activation energy, D_0 and a are constant.

Let us note that the choice of a suitable expression D is a complex problem that depends on the estimation purpose. For the industrial application underlying this study, the required residual water content at the end of the drying is quite high ($X = 1$ kg kg^{-1}) and the optimization mainly concerns the drying time and the energy consumption. It is then possible to use a simple exponential function that was shown to describe the early surface drying experimentally observed in a satisfactory way. For other applications in which very low residual solvent content is required, a more précised description of the diffusion coefficient for low moisture content should be necessary. However, as already said, the methodology presented in the following could be easily extended to other parameterization of the D.

According to the formulation of D, the inverse problem consists in estimating the vector of unknown parameters $\theta = [D_0, a, E_a]$ of the effective diffusion coefficient (Eq. 8) by minimizing an objective function taking into account the relative distance between the experimental and simulated ($\tilde{}$) values of the product mass (M) and temperature (T):

$$S(\theta) = \frac{1}{2}\sum_{i=1}^{N}\left[\alpha_i\left(M_i - \tilde{M}_i(\theta)\right)^2 + \beta_i\left(T_i - \tilde{T}_i(\theta)\right)^2\right] \tag{9}$$

where N is the number of measurements.

In this relation, weighted coefficients were introduced to have dimensionless terms. To highlight the relevance of simultaneous use of mass and temperature measurements, three kinds of tests were compared. The minimization was performed:

- by taking only mass measurements into account: $\alpha_i = \frac{1}{M_{i=0}^2}, \beta_i = 0$,
- by taking only temperature measurements into account: $\alpha_i = 0, \beta_i = \frac{1}{T_{max}^2}$,
- by combining mass and temperature measurements: $\alpha_i = \frac{1}{M_{i=0}^2}, \beta_i = \frac{1}{T_{max}^2}$.

Furthermore, to compare the three minimization procedures, two types of criteria were defined as follows:

$$Q_M(\theta) = \frac{1}{N}\sum_{i=1}^{N}\frac{\left|M_i - \tilde{M}_i(\theta)\right|}{M_i} \quad \text{and} \quad Q_T(\theta) = \frac{1}{N}\sum_{i=1}^{N}\frac{\left|T_i - \tilde{T}_i(\theta)\right|}{T_i} \tag{10}$$

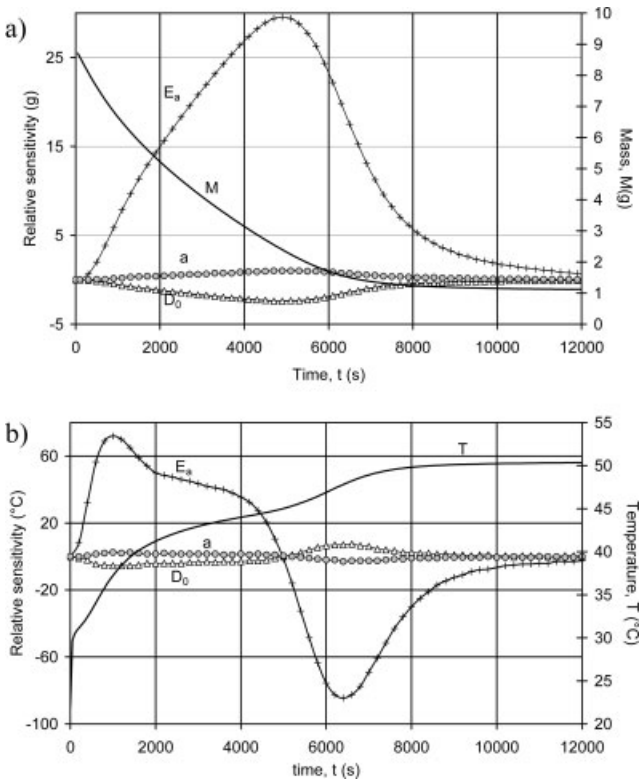

Figure 4. Relative sensitivity of mass (a) and temperature (b) for convective drying: T_{air} = 55°C, v_{air} = 2.8 m s^{-1}, H_R = 20%.

The values of the parameters were bounded. Thanks to previous results in the literature,[7,21] the activation energy of solvent/polymer system was assumed to vary between 20 and 40 kJ mol^{-1}. Parameter a is a positive constant and its maximal value was fixed to one to avoid the divergence of the diffusion coefficient for low-moisture content. To get a prior estimation of the diffusion coefficient during the first stage of drying, we used an approximate analytical model.[32,33] It was found between 10^{-10} and 10^{-11} m^2 s^{-1}.[34] As a consequence D_0 is between 4×10^{-7} and 10^{-4} m^2 s^{-1}. Furthermore, to make optimization easier, a constraint on the diffusion coefficient for high-moisture content was also introduced in the minimization procedure: $D_{t=0} \geq 10^{-11} m^2 s^{-1}$.

An iterative quadratic programming (SQP) method, suitable for solving nonlinear constrained problems, was used.[35] In this method, a sequence of quadratic programming approximations is solved and the objective function is a quadratic approximation of the Lagrangian function and is solved by a Newton method.[35]

The calculations were stopped when one following criterion is satisfied:

$$S(\theta) < E_1 \tag{11}$$

$$\left\|\theta^{j+1} - \theta^{j}\right\| < E_2 \tag{12}$$

where E_1, E_2 are prescribed tolerances, $\| \ \|$ is the Euclidean vector norm, and j the number of iteration.

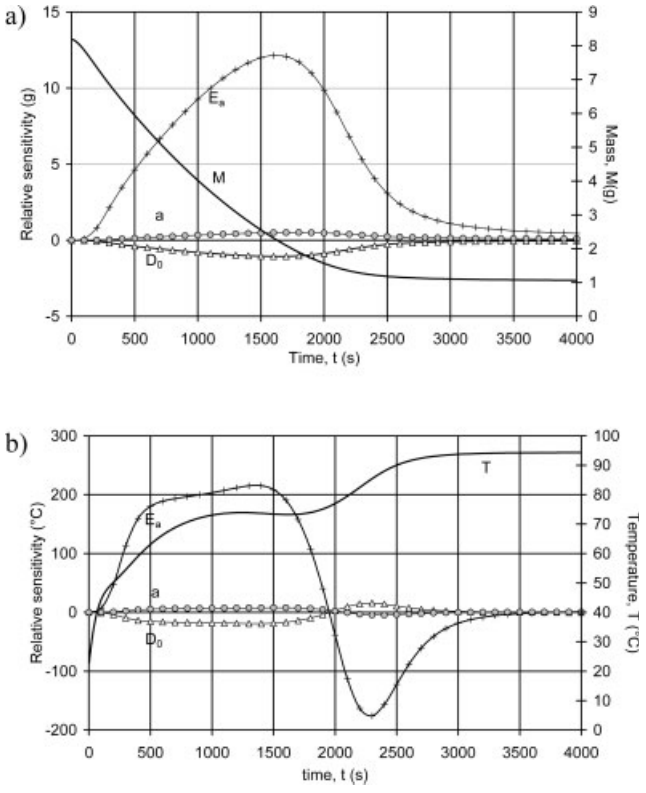

Figure 5. Relative sensitivity of mass (a) and temperature (b) for convective-infrared drying: T_{air} = 35°C, v_{air} = 1 m s^{-1}, H_R = 20%, P_{IR} = 3.7 kW m^{-2}.

Table 2. Reduced Covariance Matrices

Convective Drying			Infrared-Convective Drying		
D_0	E_a	a	D_0	E_a	a
Mass (g)					
1.0143	0.082	−0.015	9.931	0.845	0.4036
0.082	0.0066	−0.0016	0.845	0.0727	0.0335
−0.015	−0.0016	0.0161	0.4036	0.0335	0.0408
Temperature (°C)					
0.684	0.055	0.0343	1.117	0.0953	0.0805
0.055	0.0045	0.0009	0.0953	0.0081	0.0064
0.0343	0.0009	0.0758	0.0805	0.0064	0.0214

Results and Discussion

To test the estimation feasibility, a sensitivity analysis and previous tests with simulated drying kinetics were performed. Then, the method was applied to experimental mass and temperature measurements with convective and infrared-convective drying.

Sensitivity analysis

The sensitivity analysis enables to determine if it is possible to simultaneously identify the unknown parameters. Reduced sensitivity coefficients are defined as follows:

$$J_{Y,ik} = \theta_k \frac{\partial \tilde{Y}_i(\theta)}{\partial \theta_k} \tag{13}$$

where Y represents the mass or the temperature.

The values of the parameters used for numerical tests are those found by Navarri and Andrieu[21] for a PVA/water system: $D_0 = 9.38 \times 10^{-6}$ m^2 s^{-1}, E_a = 32,700 J mol^{-1}, a = 0.332. The sensitivity curves relative to mass and temperature obtained numerically by considering a small variation of parameters of $\delta = 10^{-2}$ are given for convective drying and for infrared-convective drying in Figures 4 and 5. The inputs (T_{air}, v_{air}, H_r, and P_{IR}) correspond to conditions tested during our experimental investigation. In both cases, the sensitivity of parameters D_0 and a were less than that of parameter E_a. They reached 7°C and 2.5 g for the convective drying and 18°C and 1 g for the infrared-convective drying, which is above the measurement noise estimated at ±2.5°C and ±0.2 g. However, the low sensitivity of parameter a makes it difficult to estimate. D_0 and a had higher mass sensitivities in infrared-convective drying than in convective drying. The opposite situation occurred for their temperature sensitivities. Similarly, E_a had the highest temperature sensitivity in infrared-convective drying and the highest mass sensitivity in

Table 3. Correlation Matrices

Convective Drying			Infrared-Convective Drying		
D_0	E_a	a	D_0	E_a	a
Mass (g)					
1	0.9991	0.117	1	0.9997	0.6336
0.9991	1	−0.1592	0.9997	1	0.6145
0.117	−0.1592	1	0.6336	0.6145	1
Temperature (°C)					
1	0.9944	0.1505	1	0.9998	0.521
0.9944	1	0.0493	0.9998	1	0.4814
0.1505	0.0493	1	0.521	0.4814	1

Table 4. Minimization Through Test Cases with Random Errors for Mass and Temperature

	Convective Drying			Infrared-Convective Drying		
Criterion	*M*	*T*	*M, T*	*M*	*T*	*M, T*
E_a (J mol^{-1})	32,704	32,784	32,707	32,758	32,598	32,711
a	0.336	0.287	0.321	0.318	0.355	0.328
S	9.6×10^{-5}	3×10^{-4}	4.5×10^{-4}	9×10^{-5}	1×10^{-4}	2×10^{-4}
Q_M	0.043	0.044	0.043	0.069	0.074	0.075
Q_T	0.028	0.027	0.029	0.015	0.015	0.014

convective drying. In fact, Figures 4 and 5 show that mass and temperature evolutions give complementary information for the estimation of diffusion coefficient.

With these parameters founding in literature for a PVA/water system, the isenthalpic stage is very short. It is principally due to the high value of E_a. In the studied system which is a PVA/water/glycerol blend, the isenthalpic stage appears clearly. Thus, the same sensitivity analysis was performed a posteriori, with the parameters estimated for the studied system. Results are not given here because the conclusions are roughly unchanged.

As D_0 and E_a variations seemed to be correlated, which would not allow the simultaneous estimation of these parameters, the reduced covariance and correlation matrices corresponding to D_0, E_a, and a were calculated. They are respectively defined as follows:

$$Var_Y(\theta_k, \theta_l) = \Omega_Y^2 \left(J_Y^T J_Y\right)^{-1} = \Omega_Y^2 \begin{bmatrix} \sum_{i=1}^{N} \left(J_{Y,ik}\right)^2 & \sum_{i=1}^{N} \left(J_{Y,ik} J_{Y,il}\right) \\ \sum_{i=1}^{N} \left(J_{Y,ik} J_{Y,il}\right) & \sum_{i=1}^{N} \left(J_{Y,il}\right)^2 \end{bmatrix}^{-1} \quad (14)$$

$$\mathrm{Cor}_Y(\theta_k, \theta_l) = \frac{\mathrm{Cov}(\theta_k, \theta_l)}{\sqrt{\mathrm{Var}(\theta_k)\mathrm{Var}(\theta_l)}} \quad (15)$$

Their estimation is accurate if the variances are small and if the correlation coefficients are far from one.[36] Tables 2 and 3 give the results obtained using mass and temperature reduced sensitivity. The correlation matrices showed that parameters E_a and D_0 are linearly dependent and thus cannot be simultaneously accurately estimated. This is why we chose to fix the parameter with the lowest sensitivity that is to say D_0. Thus, in the following, the unknown parameter vector is reduced to $P = [a, E_a]$.

Numerical tests

Simulated drying kinetics, using the same example as in the previous section ($D_0 = 9.38 \times 10^{-6}$ m^2 s^{-1}, $E_a = 32{,}700$ J mol^{-1}, $a = 0.332$), were used in the minimization procedure as fictive measurements to test the accuracy of the method. The initial values of the unknown parameters introduced in the optimization procedure are $E_a = 30{,}000$ J mol^{-1} and $a = 0.5$ and D_0 was fixed to its exact value. The initial values of the criteria on mass and temperature were relatively high ($Q_M = 5.3$ and $Q_T = 15.1$). The minimization procedure was tested using a criterion on mass measurement only, then on temperature measurements only and finally using both criteria. With exact data (i.e., no random noise is added to the simulated kinetics), the algorithm converged to the exact values for the three cases. Table 4 presents the results of the minimization procedure when introducing uniformly distributed random errors[37] to simulate measurement errors. In this case, the results obtained depend on the criterion. Measurement errors were more important on temperature than on mass, and so the estimation of parameters was less disturbed using mass measurements only, notably in the case of the infrared-convective drying. However, the algorithm converged toward values close to the exact values for each test.

Experimental kinetics

Table 5 presents the set of experiments retained for this study. The convective dryings (Experiments 1–4) correspond to two different air temperatures (35°C or 55°C) and two different air velocities (1 m s^{-1} and 2.8 m s^{-1}). Experiment 5 is infrared-convective drying with a low and constant infrared irradiation. In Experiments 6 and 7, the infrared irradiation, initially high, was progressively decreased during drying and was then regulated on product temperature, to avoid deformation of the Petri dish (the Petri dish temperature must be less than 90°C). Theses two experiments with varying infrared irradiation correspond to a first empirical optimization of the drying process.

In the optimization procedure, the experimental product temperature was the average of the temperatures measured at the surface of the polymer and at the upper side of the Petri dish. The estimation of the diffusion coefficient was based on several steps which will now be described.

Definition of the Objective Function. First, the minimization procedure was performed on two experiments: a

Table 5. Experiments Description

	Convective Drying				Infrared-Convective Drying		
Experiment number	1	2	3	4	5	6	7
Air velocity (m s^{-1})	2.8	1	1	2.8	1	1	1
Air temperature (°C)	55	35	55	35	35	35	35
Air humidity (%)	12	30	12	35	18	19	14
Infrared irradiation (kW m^{-2})	–	–	–	–	3.7	12.3–5.6	13.3–5.6

Table 6. Minimization Through Convective (Experiment 1) and Infrared-Convective Drying (Experiment 5) with $D_0 = 5 \times 10^{-5}$ m^2 s^{-1}

	Convective Drying			Infrared-Convective Drying		
Criterion	*M*	*T*	*M, T*	*M*	*T*	*M, T*
E_a (J mol^{-1})	31,159	30,781	30,849	33,329	30,924	31,395
a	0.94	1	1	1	1	1
S	1.4×10^{-5}	8.4×10^{-4}	8.6×10^{-4}	1.1×10^{-4}	6.7×10^{-4}	1.4×10^{-3}
Q_M	0.021	0.027	0.025	0.039	0.113	0.102
Q_T	0.037	0.034	0.035	0.117	0.049	0.051
N_{iter}	15	13	14	9	6	6
N_{func}	115	72	92	52	27	31

convective drying (Experiment 1) and an infrared-convective drying (Experiment 5). D_0 was put to 5×10^{-5} m^2 s^{-1}, which corresponds to the middle of the interval previously defined for this parameter. The initial values of parameters E_a and a were the same as those used for the sensitivity analysis (E_a = 30,000 J mol^{-1} and a = 0.5). Results are given in Table 6, with the number of iterations (N_{iter}) and the number of function evaluations (N_{func}). The least satisfactory results were obtained using only mass measurements. Indeed, as the evolution of temperature was not taken into account, there was a significant difference between simulated and experimental temperatures, notably in the case of infrared-convective drying. On the other hand, if only temperature evolution was used, the minimization converged faster and particularly with infrared-convective drying. Moreover, the evolution of mass and temperature were correctly described. However, complementary tests showed that the estimated parameters depend on the initial values of E_a and a, which was not the case when mass and temperature evolution was simultaneously estimated. Then, in the following, we chose to use the objective function taking mass and temperature into account.

Fixed value of the Parameter D_0. The second step consists of investigating the inverse method for different values of D_0. The same two experiments are used. With a criterion for mass and temperature, regardless of the initial value of the parameters, the algorithm always converged toward a value of 1 for parameter a. As they are correlated, the estimated value of E_a depends on the value of D_0. However, for a given D_0 and for each initial value of E_a, the algorithm converged toward similar values of the activation energy. The final objective function is about 10^{-3} for all the performed tests. In the following, we use $D_0 = 8 \times 10^{-7}$ m^2 s^{-1} that corresponds to the smallest objective function.

Estimation. First, the values of a and E_a were estimated by using only one experiment (Experiment 1 or 5). As can be seen in Table 7, the estimated parameters are very close. The estimation required less iterations with the infrared-convective drying, but the objective function was smaller with

Table 7. Minimization Through Convective (Experiment 1) and Infrared-Convective Drying (Experiment 5) with $D_0 = 8 \times 10^{-7}$ m^2 s^{-1}

	Convective Drying	Infrared-Convective Drying
Air velocity, v_{air} (m s^{-1})	2.8	1.0
Air temperature, T_{air} (°C)	55	35
Infrared irradiation, P_{IR} (kW m^{-2})	–	3.7
E_a (J mol^{-1})	20,430	20,379
a	1	1
S	6.86×10^{-4}	1.3×10^{-3}
Q_M	0.016	0.095
Q_T	0.035	0.049
N_{iter}	11	7
N_{func}	71	31

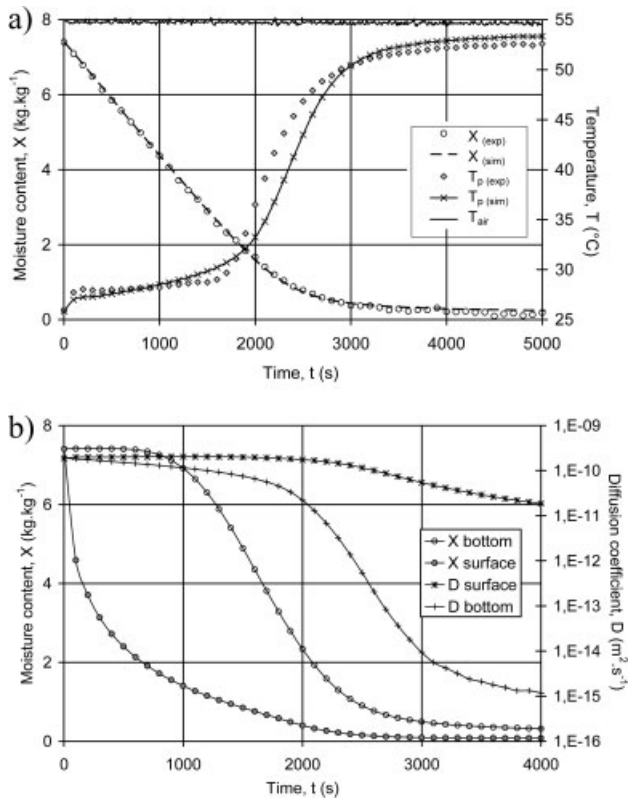

Figure 6. Simulated and experimental kinetics (a) and evolution of moisture content and diffusion coefficient at the surface and at the bottom of the product as a function of time (b) for convective drying: T_{air} = 55°C, v_{air} = 2.8 m s^{-1}, H_R = 11%.

the convective drying since the mass evolution is better described (Q_M is smaller). Figure 6 presents the results of the minimization through convective drying (Experiment 1). The average error for mean moisture content is less than 0.2 kg kg^{-1}. It corresponds to an error for mass inferior to the standard deviation of measurements. During the first stage of the drying, the temperature evolution is well fitted with the model. A small discrepancy is observed during the transitional stage, in which the simulated temperature is lower than the experimental one. The average difference is 1°C with a standard deviation of 0.85°C. As can be seen in Figure 6b, the diffusion coefficient and the moisture content quickly decrease at the surface. Results obtained with the infrared-convective drying test (Experiment 5) are given in Figure 7. The moisture content evolution is satisfactory. Although the temperature evolution is globally well described, we can note that the temperature is slightly overestimated during the first stage of drying. This result can be explained by the uncertainty of the absorbed infrared irradiation in the product. Comparing Figures 6 and 7, we can see that the drying is much faster with the infrared drying, which corresponds to a fast drying of the surface of the product experimentally observed and well captured by the model.

Several complementary tests were performed to test the algorithm. For example, the criterion minimization was performed through Experiments 1 and 5 by introducing an error of 10% into the heat convective exchange coefficient. The algorithm converged towards the value of E_a and a indicated in Table 7 with a relative error inferior to 1%, which is very satisfactory. Concerning the time horizon used to perform the criterion minimization (i.e., N, the number of measurements in Eq. 9), a good compromise was obtained by using measurements up to a global moisture content of about 0.3 kg kg^{-1}. Indeed, the expression used to describe the variation of the diffusion coefficient with water content diverges for small moisture content.

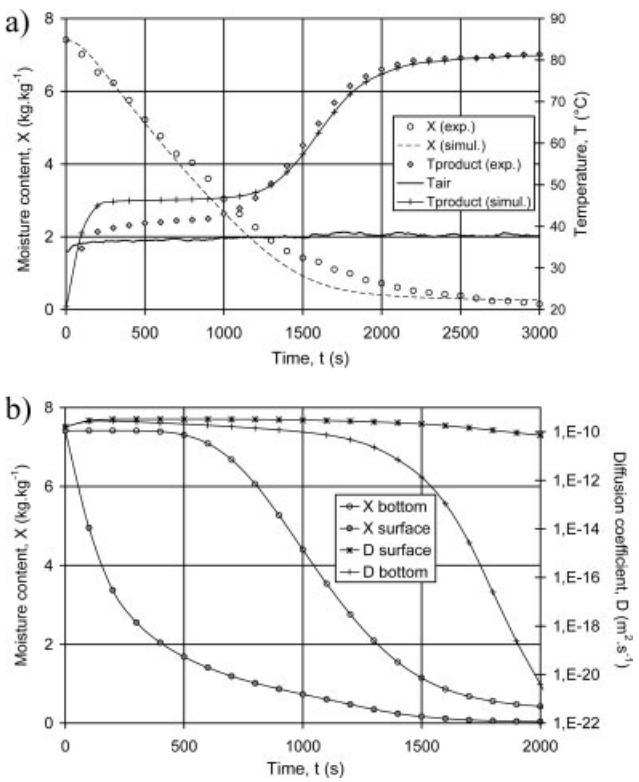

Figure 7. Simulated and experimental kinetics (a) and evolution of moisture content and diffusion coefficient at the surface and at the bottom of the product as a function of time (b) for infrared-convective drying: T_{air} = 35°C, v_{air} = 1 m s^{-1}, H_R = 18%, P_{IR} = 3.7 kW m^{-2}.

Validation. These preliminary tests were performed on a convective and an infrared convective drying experiments (Experiment 1 and 5). To test the robustness and validity domain of the estimation, several tests were performed on the other experiments.

First, the same minimization procedure was used on the three other convective heating experiments, i.e., Experiments 2, 3, and 4 in Table 5. In Experiment 2, the lower air velocity (v_{air} = 1 m s^{-1}) explains the longer drying time. The drying time used for the minimization was 7000 s and the estimated parameters are a = 1 and E_a = 21,457 J mol^{-1} with Q_M = 4.7% and Q_T = 2.3%. For Experiment 3, the minimization carried out up to 11,000 s leads to a = 1 and E_a = 21,710 J mol^{-1} with Q_M = 6% and Q_T = 2.6%. Then, in the last experiment (v_{air} = 1 m s^{-1}, T_{air} = 35°C), the minimization performed up to 12,000 s converged toward a = 1 and E_a = 21,558 J mol^{-1}. Thus, it seems that for these three convective experiments, the minimization procedure converged toward a similar set of parameters.

To confirm the validity of the estimated effective diffusion coefficient for this experimental configuration, Figure 8 compares the experimental and simulated drying kinetics, using the set of parameter deduced from Experiments 1 and 5. For all the Experiments 1 to 5, the agreement between experimental and simulated mass and temperature is rather satisfactory with $Q_M < 8\%$ and $Q_T < 3\%$. Then we can conclude that the estimated diffusion coefficient is suitable to get a good evaluation of temperature and mass evolutions for convective drying and infrared-convective drying with small infrared irradiation, and thus could be used to optimize the drying process.

Let us now consider the last two Experiments 6 and 7. They correspond to infrared-convective drying with initial high infrared irradiations (respectively 12.3 kW m^{-2} and 13.3 kW m^{-2}). As already said in the experimental section, infrared irradiation has to be progressively decreased and then regulated on the sample temperature to avoid passing 90°C. Despite this regulation, great and numerous stria were observed at the surface and experimental kinetics showed that the mass stayed constant. The used model is thus not valid any more for this part of the drying. The minimization was only performed on the beginning of the drying that is to say up to 900 s for Experiment 6 and up to 500 s for Experiment 7. The estimated values are, respectively, a = 1, E_a = 20,574 J mol^{-1} for Experiment 6 and a = 0.93 and E_a = 20,447 J mol^{-1} for Experiment 7. The obtained values are close to previous estimated parameters. As can be seen in Figure 8, the temperature evolution is satisfactory, but the model underestimates the moisture content at the end of the drying, in which the experimental

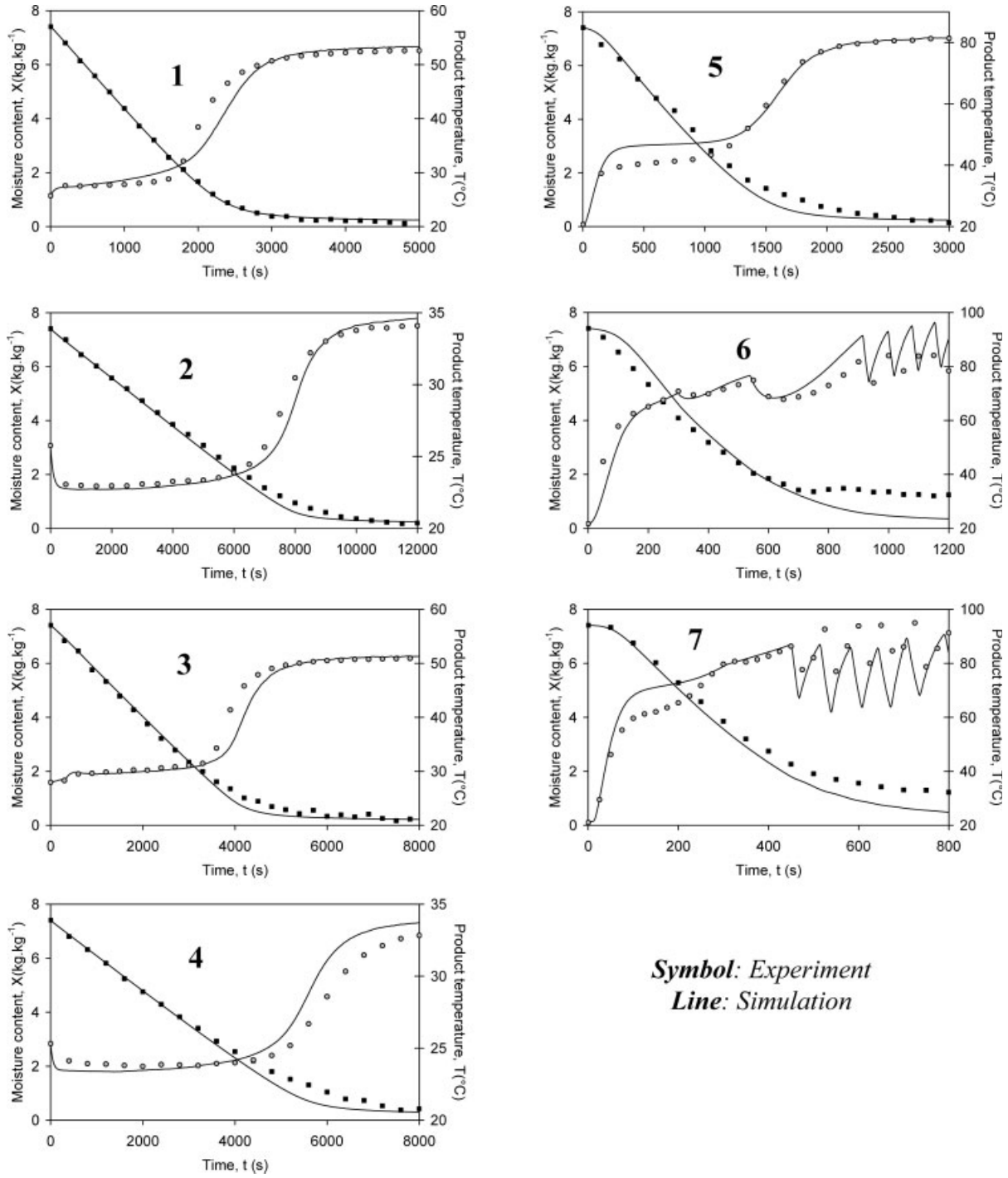

Figure 8. Experimental and simulated drying kinetics with $D_0 = 8 \times 10^{-7}$ m^2 s^{-1}, $a = 1$ and $E_a = 20{,}428$ J mol^{-1} of convective drying (1,2,3,4) and infrared-convective drying (5,6,7) experiments described in Table 5.

configuration is beyond the validity domain of the estimation procedure.

Conclusion

This study deals with the estimation of an effective diffusion coefficient of an aqueous PVA solution by an inverse method. A model based on a barycentric approach was retained to obtain an accurate simulation of the moisture content and temperature of the product during drying. An exponential expression of the evolution of diffusion coefficient with moisture content and temperature was used, with only three unknown parameters. A minimization procedure taking into account mass and temperature evolution

was established and the feasibility of the method was first numerically tested. The validity domain of the estimation was investigated, using different experimental configurations.

Future developments will concern the understanding of the sample behavior for high infrared heating and the use of this model in its validity domain to determine an optimal law for the infrared irradiation in order to find a suitable compromise between drying time, energy consumption, and product quality.

Notation

Roman letters

a = diffusion coefficient parameter
a_w = water activity
C_p = specific heat capacity, J(kg K)$^{-1}$
D = water diffusion coefficient, m^2 s^{-1}
D_0 = diffusion coefficient parameter, m^2 s^{-1}
e = thickness, m
E_a = activation energy, J mol^{-1}
F_m = drying rate, kg m^{-2} s^{-1}
h_p = heat convective exchange coefficient, W m^{-2} K^{-1}
H_R = relative humidity, %
k_m = mass-transfer coefficient, m s^{-1}
M_v = molecular weight, kg mol^{-1}
N = number of experimental data
P = irradiation, W m^{-2}
P_t = atmospheric pressure, Pa
P_v = water vapour pressure, Pa
R = gas constant, J(K mol)$^{-1}$
t = time, s
T = temperature, °C
v = velocity, m s^{-1}
X = moisture content (dry basis), kg kg^{-1}
z = spatial coordinates

Greek letters

ϕ = heat flow, W m^{-2}
Ω = measurement noise
σ = Stefan-Boltzmann constant; W m^{-2} K^{-4}
ε = product emissivity
ξ = dimensionnless space coordinates
λ = thermal conductivity, W(m K)$^{-1}$
ρ = density, kg m^{-3}
ψ = linear shrinkage coefficient
ζ = space coordinate, m

Subscripts

A = water constituent
B = polymer constituent
b = Petri dish
d = dried product
IR = infrared
M = mass
t = total
T = temperature
sat = saturated

Literature Cited

1. Mujumdar AS. *Handbook of Industrial Drying*, 3rd Edition. New York: CRC Press/Taylor & Francis; 2006:953–979.
2. Ludwig I, Schabel W, Kind M, Castaing J-C, Ferlin P. Drying and film formation of industrial waterborne latices. *AIChE J*. 2007; 53:3.
3. Alsoy S, Duda JL. Drying of solvent coated polymer films. *Dry Technol*. 1998;16:15–44.
4. Cairncross RA, Durning CJ. Modeling drying of viscoelastic polymer coatings. *AIChE J*. 1996;42:55–67.
5. Vinjamur M, Cairncross RA. Non-Fickian nonisothermal model for drying of polymer coatings. *AIChE J*. 2002;11:2444–2458.
6. Chen XD. Moisture diffusivity in food and biological materials. *In the 15th International Drying Symposium*, Budapest, Hungary, August 20–23, 2006, Mujumdar AS, Series Editor, Vol. A.: 18–27.
7. Dufour P, Toure Y, Blanc D, Laurent P. On nonlinear distributed parameter model predictive control strategy: on-line calculation time reduction and application to an experimental drying process. *Computers Chem Eng*. 2003;27:1533–1542.
8. Okazaki M, Shioda K, Masuda K, Toei R. Drying mechanism of coated film of polymer solution. *J Chem Eng Japan*. 1974;7:99–105.
9. Loulou T, Adhikari B, Lecomte D. Estimation of concentration-dependent diffusion coefficient in drying process from the space-averaged concentration versus time with experimental data. *Chem Eng Sci*. 2006;61:7185–7198.
10. Dantas LB, Orlande HRB, Cotta RM. An inverse problem of parameter estimation for heat and mass transfer in capillary porous media. *Int J Heat Mass Transfer*. 2003;46:1587–1598.
11. Price PE, Cairncross RA. Optimization of single-zone drying of polymer solution coatings using mathematical modeling. *J Appl Polym Sci*. 2000;78:149–165.
12. Wang R, Wang Q, Li L. Evaporation behavior of water and its plasticizing effect in modified poly(vinyl alcohol) systems. *Polym Int*. 2003;52:1820–1826.
13. Allanic N. *Optimization with Constraints of a Drying Combining Convective Exchanges and Infrared Radiation Technologies—Application to a Polymer in Aqueous Solution, PhD Thesis*. Lorient, France: Université de Bretagne Sud, 2006.
14. Basu S, Shivhare US, Mujumdar AS. Models for sorption isotherms for foods: a review. *Dry Technol*. 2006;24:917–930.
15. Allanic N, Salagnac P, Glouannec P. Convective and radiant drying of a polymer aqueous. *Heat Mass Transfer*. 2006;43:1087–1095.
16. Glouannec P, Lecharpentier D, Noel H. Experimental survey on the combination of radiating infrared and microwave sources for the drying of porous material. *Appl Thermal Eng*. 2002;22:1689–1703.
17. Vrentas JS, Vrentas CM. Drying of solvent-coated polymer films. *J Polym Sci Part B: Polym Phys*. 1994;32:187–194.
18. Bird RB, Stewart WE, Lightfoot EN. *Transport Phenomena*, 2nd edition. New York: Wiley, 2002.
19. Camacho J, Brenner H. On convection induced by molecular diffusion. *Ind Eng Chem Res*. 1995;34:3326–3335.
20. Brenner H. Kinematics of volume transport. *Phys A*. 2005;349:11–59.
21. Navarri P, Andrieu J. High-intensity infrared drying study. II. Case of thin coated films. *Chem Eng Process*. 1993;32:319–325.
22. Alsoy S, Duda JL. Modeling of multicomponent drying of polymer films. *AIChE J*. 1999;45:896–905.
23. Guerrier B, Bouchard C, Allain C, Bénard C. Drying kinetics of polymers films. *AIChE J*. 1998;44:791–798.
24. Incropera FP, DeWitt DP, Bergman TL, Lavine A. *Fundamentals of Heat and Mass Transfers*, 6th edition. New York: Wiley, 2005.
25. Patankar SV. *Numerical Heat Transfer and Fluid Flow*. New York: Hemisphere Publishing Corporation, 1980.
26. Carnahan B, Luther HA, Wilkes JO. *Applied Numerical Methods*. Florida: Krieger Publishing Company Malabar, 1990.
27. Yoshida M, Miyashita H. Drying behavior of polymer solution containing two volatile solvents. *Chem Eng J*. 2002;86:193–198.
28. Vrentas JS, Vrentas CM. Predictive methods for self-diffusion and mutual diffusion coefficients in polymer/solvent systems. *Eur Polym J*. 1998;34:797–803.
29. Frias J, Olivieira JC, Schittkowski K. Modeling and parameter identification of a maltodextrin DE 12 drying process in a convection oven. *Appl Math Model*. 2001;25:449–462.
30. Ngui MO, Mallapragada SK. Understanding isothermal semicrystalline polymer drying: mathematical models and experimental characterization. *J Polym Sci Part B: Polymer Phys*. 1998;36:2771–2780.

31. Wong SS, Altinkaya SA, Mallapragada SK. Drying of semicrystalline polymers: mathematical modeling and experimental characterization of poly(vinyl alcohol) films. *Polymer*. 2004;45:5151–5161.
32. Livian I, Vergnaud JM. Process of drying a polymeric paint by diffusion-evaporation and shrinkage. Determination of the concentration-dependent diffusivity. *Polym Test*. 1995;14:479–487.
33. Mintzlaff J. Determination of properties for the calculation of aqueous thin film drying. *Heat Mass Transfer*. 2001;37:617–622.
34. Allanic N, Salagnac P, Glouannec P. Estimation of diffusion coefficient in drying of polymer aqueous solution. *In the 15th International Drying Symposium*, Budapest, Hungary, August 20–23, 2006.
35. Edgar TF, Himmelblau DM, Lasdon LS. *Optimization of Chemical Processes*, 2nd edition. Boston: McGraw-Hill, 2001.
36. Remy B, Degiovanni A. Parameters estimation and measurement of thermophysical properties of liquids. *Int J Heat Mass Transfer*. 2005;48:4103–4120.
37. Li F, Niu J. An inverse approach for estimating the initial distribution of volatile organic compounds in dry building material. *Atmos Environ*. 2005;39:1447–1455.

Manuscript received Dec. 27, 2007, revision received Dec. 1, 2008, and final revision received Feb. 12, 2009.